

# SOLITON SPLITTING BY EXTERNAL DELTA POTENTIALS

JUSTIN HOLMER, JEREMY MARZUOLA, AND MACIEJ ZWORSKI

**ABSTRACT.** We show that a soliton scattered by an external delta potential splits into two solitons and a radiation term. Theoretical analysis gives the amplitudes and phases of the reflected and transmitted solitons with errors going to zero as the velocity of the incoming soliton tends to infinity. Numerical analysis shows that this asymptotic relation is valid for all but very slow solitons.

We also show that the total transmitted mass, that is the square of the  $L^2$  norm of the solution restricted on the transmitted side of the delta potential is in good agreement with the quantum transmission rate of the delta potential.

## 1. INTRODUCTION AND STATEMENT OF RESULTS

A bright soliton is a travelling wave solution,

$$(1.1) \quad u(x, t) = A \operatorname{sech}(A(x - vt)) \exp(i\varphi + ivx + i(A^2 - v^2)t/2), \quad A > 0, \quad v \in \mathbb{R},$$

of the nonlinear Schrödinger equation (NLS):

$$(1.2) \quad i\partial_t u + \frac{1}{2}\partial_x^2 u + u|u|^2 = 0$$

Its remarkable feature is total coherence – see for instance [11] for a review of theoretical and experimental situations in which bright solitons arise.

Suppose now that we consider a perturbed NLS, that is, the Gross-Pitaevskii equation, by adding an external potential:

$$(1.3) \quad \begin{cases} i\partial_t u + \frac{1}{2}\partial_x^2 u - q\delta_0(x)u + u|u|^2 = 0 \\ u(x, 0) = u_0(x) \end{cases}$$

If as initial data we take a soliton approaching the impurity from the left:

$$(1.4) \quad u_0(x) = e^{ivx} \operatorname{sech}(x - x_0), \quad x_0 \ll 0,$$

then until time  $t_0 \approx x_0/v$ , the propagation will still be approximately given by (1.1). Here we put  $A = 1$  and  $\varphi = 0$ . Scaling properties of the delta function show that this allows general soliton initial conditions. Thus the velocity,  $v$ , and the coupling constant,  $q$ , are the only parameters of the problem.

For  $t > x_0/v$  the effects of the delta potential are dramatically visible and as we show in this paper they can be understood using the transmission and reflection coefficients of the delta potential from standard scattering theory.

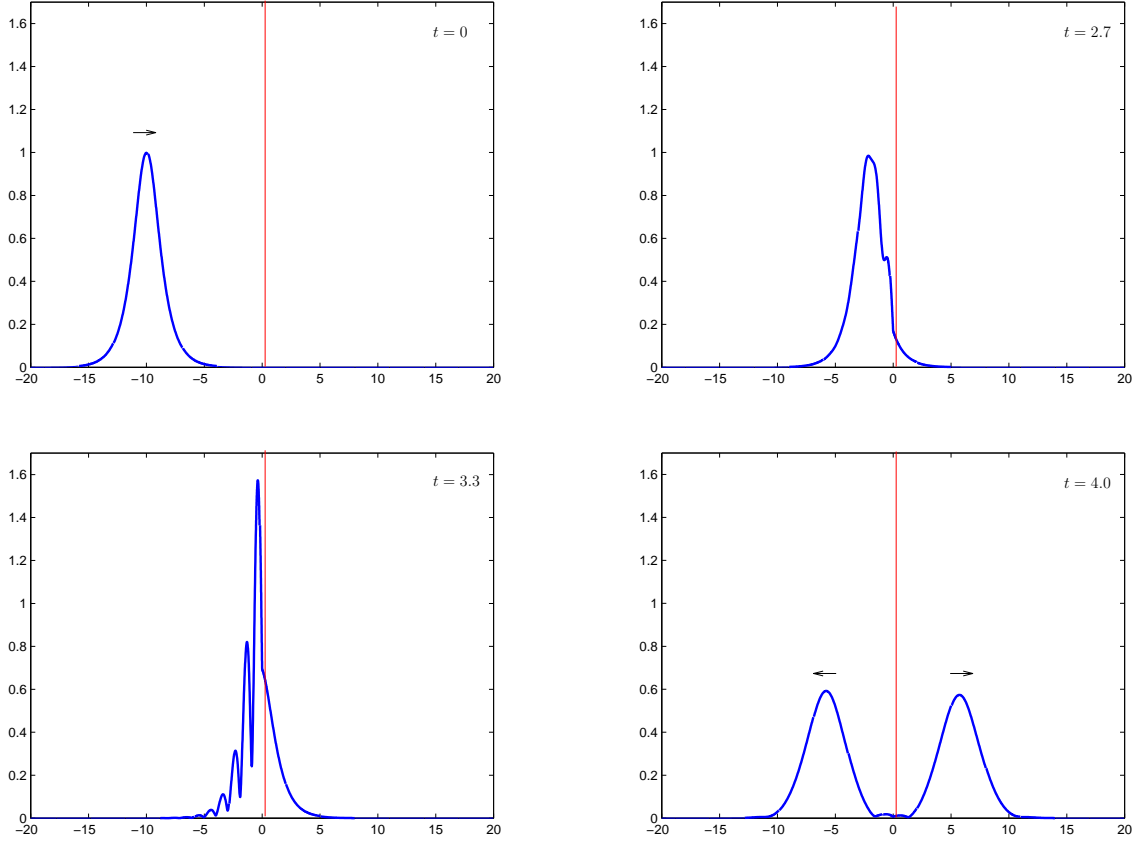


FIGURE 1. Numerical simulation of the case  $q = v = 3$ ,  $x_0 = -10$ , at times  $t = 0.0, 2.7, 3.3, 4.0$ . Each frame is a plot of amplitude  $|u|$  versus  $x$ .

For the soliton scattering the natural definition of the transmission rate is given by

$$(1.5) \quad T_q^s(v) = \frac{1}{2} \lim_{t \rightarrow \infty} \int_0^\infty |u(t, x)|^2 dx, \quad \int_{\mathbb{R}} |u(t, x)|^2 dx = 2,$$

where on the right we recalled the conservation of the  $L^2$  norm. The reflection coefficient is

$$(1.6) \quad R_q^s(v) = \frac{1}{2} \lim_{t \rightarrow \infty} \int_{-\infty}^0 |u(t, x)|^2 dx,$$

and  $T_q^s(v) + R_q^s(v) = 1$ .

The following result is obtained by a numerical analysis of the problem:

$$(1.7) \quad T_q^s(v) = \frac{v^2}{v^2 + q^2} + \mathcal{O}\left(\frac{1}{v^2}\right).$$

In §4 we explain how a weaker rigorous result is obtained in [10, Theorem 1]. Fig.2 shows the numerical agreement of  $T_q^s(v)$  as a function of  $\alpha = q/v$ .

The leading term on the right hand side of (1.7) has the following natural interpretation in elementary scattering theory, see for instance [12]. Since we need it below to formulate the result about soliton splitting (1.11) we review the basic concepts. Thus let

$$H_q = -\frac{1}{2} \frac{d^2}{dx^2} + q \delta_0(x),$$

and consider a general solution to  $(H_q - \lambda^2/2)u = 0$ ,

$$u(x) = A_{\pm} e^{-i\lambda x} + B_{\pm} e^{i\lambda x}, \quad \pm x > 0.$$

The matrix

$$S(\lambda) : \begin{bmatrix} A_+ \\ B_- \end{bmatrix} \mapsto \begin{bmatrix} A_- \\ B_+ \end{bmatrix},$$

is called the *scattering matrix* and in our simple case it can be easily computed:

$$S(\lambda) = \begin{bmatrix} t_q(\lambda) & r_q(\lambda) \\ r_q(\lambda) & t_q(\lambda) \end{bmatrix},$$

where  $t_q$  and  $r_q$  are the transmission and reflection coefficients:

$$(1.8) \quad t_q(\lambda) = \frac{i\lambda}{i\lambda - q}, \quad r_q(\lambda) = \frac{q}{i\lambda - q}.$$

They satisfy two equations, one standard (unitarity) and one due to the special structure of the potential:

$$(1.9) \quad |t_q(\lambda)|^2 + |r_q(\lambda)|^2 = 1, \quad t_q(\lambda) = 1 + r_q(\lambda).$$

The quantum transmission rate at velocity  $v$  is given by the square of the absolute value of the transmission coefficient (1.8),

$$(1.10) \quad T_q(v) = |t_q(v)|^2 = \frac{v^2}{v^2 + q^2}.$$

We recall (see [10, (2.21)]) that if  $\psi$  is a smooth function which is zero outside, say,  $[-a, -b]$ ,  $a > b > 0$ , then

$$\int_0^\infty |\exp(-itH_q)\psi(x)|^2 dx = T_q(v) + \mathcal{O}\left(\frac{1}{v^2}\right),$$

just as in the nonlinear soliton experiment (1.7).

Hence (1.7) shows that in scattering of fast solitons the transmission rate is well approximated by the quantum transmission rate of the delta potential – see §2 for more on that and the comparison with the linear case.

Our second result shows that the scattered solution is given by a sum of a reflected and a transmitted soliton, and of a time decaying (radiating) term. In other words, the delta potential splits the incoming soliton into two waves which become single *solitons*. In

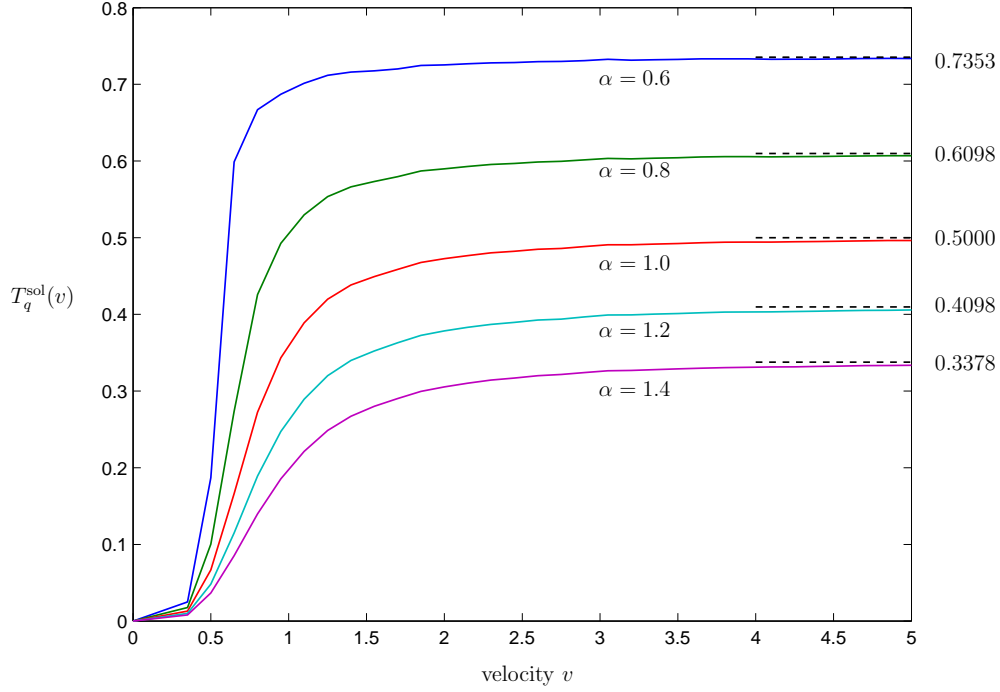


FIGURE 2. The figure illustrates the convergence, as  $v \rightarrow \infty$ , of  $T_q^{\text{sol}}(v)$  to the expected asymptotic value  $1/(1 + \alpha^2)$  for  $\alpha = +0.6, +0.8, \dots, +1.4$  (so  $q > 0$ ). It shows that the large velocity asymptotic behaviour in fact takes hold by velocity  $v \sim 3$ .

previous works in the physics literature (see for instance [5]) the resulting waves were only described as “soliton-like”. More precisely, for  $t \gg |x_0|/v$  we have

$$\begin{aligned}
 (1.11) \quad u(x, t) &= u_T(x, t) + u_R(x, t) + \mathcal{O}_{L_x^\infty} \left( (t - |x_0|/v)^{-1/2} \right) + \mathcal{O}_{L_x^2}(v^{-2}), \\
 u_T(x, t) &= e^{i\varphi_T} e^{ixv + i(A_T^2 - v^2)t/2} A_T \operatorname{sech}(A_T(x - x_0 - tv)), \\
 u_R(x, t) &= e^{i\varphi_R} e^{-ixv + i(A_R^2 - v^2)t/2} A_R \operatorname{sech}(A_R(x + x_0 + tv)),
 \end{aligned}$$

where

$$A_T = \begin{cases} 2|t_q(v)| - 1, & |t_q(v)| \geq 1/2 \\ 0, & |t_q(v)| \leq 1/2, \end{cases} \quad A_R = \begin{cases} 2|r_q(v)| - 1, & |r_q(v)| \geq 1/2 \\ 0, & |r_q(v)| \leq 1/2, \end{cases}$$

and

$$\begin{aligned}
 \varphi_T &= \arg t_q(v) + \varphi_0(|t_q(v)|) + (1 - A_T^2)|x_0|/2v, \\
 \varphi_R &= \arg r_q(v) + \varphi_0(|r_q(v)|) + (1 - A_R^2)|x_0|/2v,
 \end{aligned}$$

$$\varphi_0(\omega) = \int_0^\infty \log \left( 1 + \frac{\sin^2 \pi \omega}{\cosh^2 \pi \zeta} \right) \frac{\zeta}{\zeta^2 + (2\omega - 1)^2} d\zeta.$$

Here  $t_q(v)$  and  $r_q(v)$  are the transmission and reflection coefficients of the delta-potential (see (1.8)).

The result is illustrated in Fig.3. We can consider  $A_R(q/v)$  and  $A_T(q/v)$  as nonlinear replacements of  $R_q(v)$  and  $T_q(v)$ , respectively. Clearly  $A_T + A_R \neq 1$  except in the asymptotic limits  $q/v \rightarrow 0, \infty$ . Thus if we consider soliton scattering “particle-like” it is nonelastic.

In Fig.3 we also see the thresholds for the formation of reflected and transmitted solitons:

$$(1.12) \quad \begin{aligned} v \leq |q|/\sqrt{3} &\implies \text{no transmitted soliton } u_T, \\ v \geq \sqrt{3}|q| &\implies \text{no reflected soliton } u_R. \end{aligned}$$

Scattering of solitons by delta impurities is a natural model explored extensively in the physics literature – see for instance [5],[9], and references given there. The heuristic insight that at high velocities “linear scattering” by the external potential should dominate the partition of mass is certainly present there. It would be interesting to see if bright solitons seen in Bose-Einstein condensates [1] could be “split” using lasers modeled by delta impurities<sup>1</sup>.

In the mathematical literature the dynamics of solitons in the presence of external potentials has been studied in high velocity or semiclassical limits following the work of Floer and Weinstein [8], and Bronski and Jerrard [4]. Roughly speaking, the soliton evolves according to the classical motion of a particle in the external potential. That is similar to the phenomena in other settings, such as the motion of the Landau-Ginzburg vortices.

The possible novelty in (1.7) and (1.11) lies in seeing *quantum* effects of the external potential strongly affecting soliton dynamics. The rest of the paper is organized as follows. In §2 we present a more detailed discussion of numerical results, and in §3 we outline the methods used in our computations. Finally in §4 we discuss weaker but mathematically rigorous versions of (1.7) and (1.11) and give basic ideas behind the proofs.

## 2. NUMERICAL RESULTS

We now give numerical evidence for the results presented in §1: the asymptotics (1.7) and (1.11). We stress that the rigorous results of [10] provide weaker error estimates and hold in a limited time range only. We find it very interesting however that some results which are theoretically demonstrated, such as the thresholds (1.12) or the long time behaviour of the the free NLS, are difficult to verify numerically – see §§2.2 and 2.3. On the other hand things which are hard to prove, such as the existence of limits (1.5), seem to be very clear in numerical analysis.

---

<sup>1</sup>That this might be related to the topic of this paper was suggested to the authors by N. Berloff.

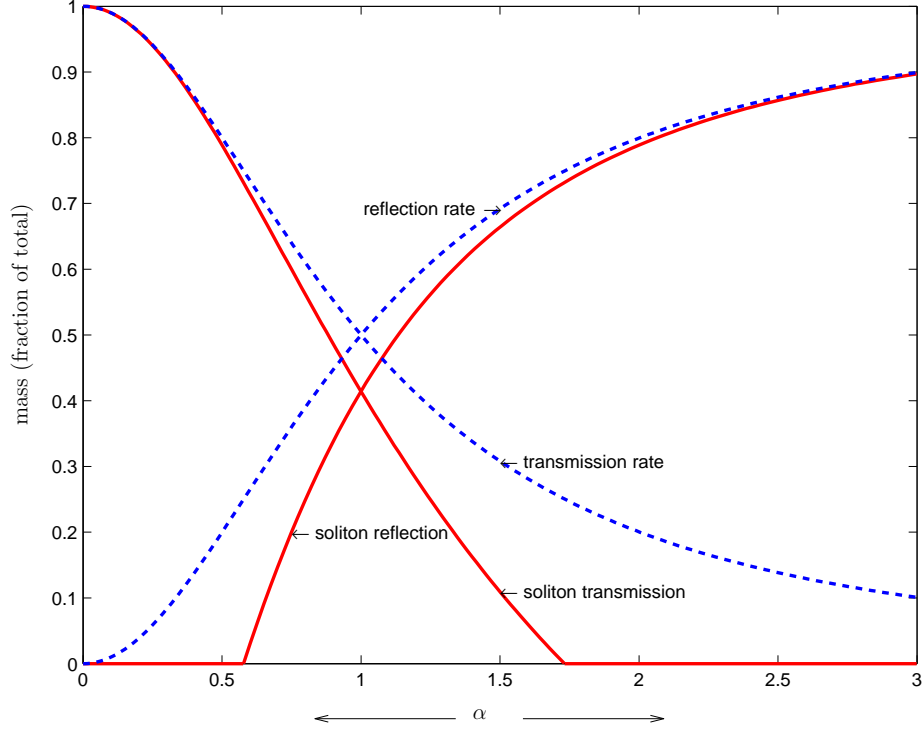


FIGURE 3. A comparison of the linear and nonlinear (soliton) scattering rates as functions of  $\alpha = q/v$ .

**2.1. Asymptotics for the transmission and trapped rates.** We recall from §1 the definitions of the transmission and reflection rates

$$T_q^s(v) = \frac{1}{2} \lim_{t \rightarrow +\infty} \int_{1/2}^{+\infty} |u(x, t)|^2 dx$$

$$R_q^s(v) = \frac{1}{2} \lim_{t \rightarrow +\infty} \int_{-\infty}^{-1/2} |u(x, t)|^2 dx.$$

These definitions assume the existence of the limits. The numerical evidence strongly supports that the limits indeed exist. We also define the trapped rate

$$B_q^s(v) = \frac{1}{2} \lim_{t \rightarrow +\infty} \int_{-1/2}^{+1/2} |u(x, t)|^2 dx$$

We have

$$B_q^s(v) = 0, \quad q \geq 0.$$

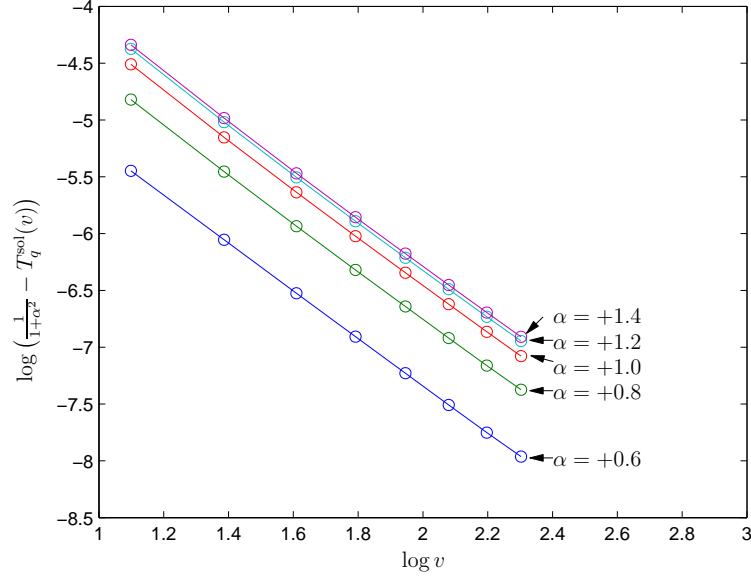


FIGURE 4. This graph is a log-log plot showing that measured values of  $T_q^s(v)$  for  $v = 3, 4, \dots, 10$  conform well to the asymptotic formula (2.3).

$\alpha$	$a(\alpha)$	$b(\alpha)$	$\alpha$	$a(\alpha)$	$b(\alpha)$
0.6	0.0415	2.0786	-0.6	0.0441	2.1076
0.8	0.0748	2.0788	-0.8	0.0761	2.0873
1.0	0.1007	2.0788	-1.0	0.1014	2.0823
1.2	0.1147	2.0778	-1.2	0.1151	2.0798
1.4	0.1185	2.0762	-1.4	0.1189	2.0776

TABLE 1. The left table gives the regression coefficients for (2.3) for  $q > 0$ , and the right table for (2.3) for  $q < 0$  – see (2.3) for the definitions of  $a(\alpha)$  and  $b(\alpha)$ ,  $\alpha = q/v$ .

However,  $B_q^s(v) > 0$  for  $q < 0$  due to the presence of a bound state at  $\lambda = -iq$  for the linear operator  $H_q$ :

$$(2.1) \quad \phi(x) = \sqrt{2|q|} e^{q|x|}.$$

The nonlinear problem has a bound state as well [5],[9]:

$$(2.2) \quad u(x, t) = e^{i\lambda^2 t/2} \lambda \operatorname{sech}(\lambda|x| + \tanh^{-1}(|q|/\lambda)), \quad 0 < \lambda < |q|.$$

This bound state is “left behind” after the interaction. The parameter  $\lambda$  depends on the initial condition.

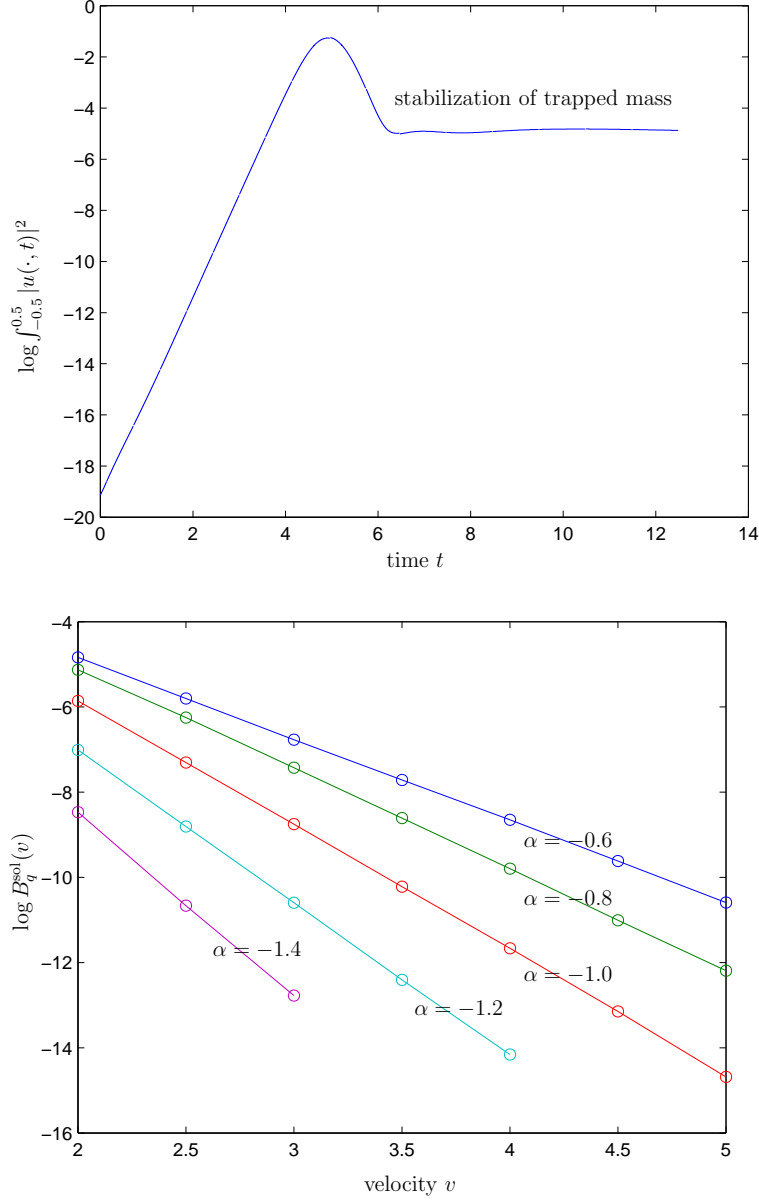


FIGURE 5. The first plot shows, for  $\alpha = -0.6$ ,  $v = 2$ ,  $x_0 = -10$ , the stabilization of the value of  $\int_{-0.5}^{0.5} |u(x, t)|^2 dx$  (which enters into the definition of  $B_q^s(v)$ ) after the interaction. The second plot shows that the measured value of  $B_q^s(v)$  for velocities  $v = 2.0, 2.5, \dots, 5.0$  conforms well to the asymptotic formula (2.4). The values of  $B_q^s(v)$  that are  $< e^{-14}$  cannot be measured with adequate precision, and thus the data for  $|\alpha| \geq 1.2$  is limited.



$\alpha$	$d(\alpha)$	$f(\alpha)$
-0.6	0.3610	1.9121
-0.8	0.6952	2.3619
-1.0	1.0328	2.9331
-1.2	1.1506	3.5784
-1.4	1.1351	4.3054

TABLE 2. Numerical results for the parameters in (2.4) for  $q < 0$ .

In both the  $q > 0$  and  $q < 0$  cases,  $T_q^s(v)$  is numerically shown to follow an asymptotic

$$(2.3) \quad T_q^s(v) \sim \frac{1}{1 + \alpha^2} - \frac{a(\alpha)}{v^{b(\alpha)}}, \quad \alpha = \frac{q}{v}.$$

Fig.4 is a log-log plot of data for velocities 3 to 10 and  $\alpha = +0.6$  to  $+1.4$ . Results of linear regression on the subset of the data for velocities 5 to 10 yields the values of  $a(\alpha)$  and  $b(\alpha)$  reported in Table 1. We see that the value of  $b(\alpha)$  displays little variation with  $\alpha$  and is approximately 2.07. When the regression is performed on the subset of the data for velocities 8 to 10, the values of  $b(\alpha)$  obtained are approximately 2.05 leading us to conjecture that the true value of  $b(\alpha)$  is exactly 2, as stated in (1.7).

The data for  $q < 0$  gives a plot nearly identical to Fig.4 owing to the exponential decay of the trapped mass  $B_q^s(v)$  (discussed below). The values of  $a(\alpha)$  and  $b(\alpha)$  obtained from the  $q < 0$  data are also reported in Table 1, and we still expect that the true value of  $b(\alpha)$  is 2.

Another feature apparent in Fig.4 and Table 1 is that the value of  $a(\alpha)$  stabilizes as  $\alpha \rightarrow \infty$  (note the proximity of the lines for  $\alpha = 1.2$  and  $\alpha = 1.4$  in Fig.4). This feature coincides with our analytical result, which establishes a (nonoptimal) bound on the asymptotic of  $v^{-1/2+}$ , independent of  $\alpha$ .

The trapped mass coefficient  $B_q^s(v)$ , on the other hand, decays exponentially.

$$(2.4) \quad B_q^s(v) \sim d(\alpha)e^{-f(\alpha)v}, \quad \alpha = \frac{q}{v}.$$

The second frame of Fig.5, which presents data for velocities 2 to 5 and  $\alpha = -0.6$  to  $-1.4$ , demonstrates that  $B_q^s(v)$  conforms well to the formula (2.4). Linear regression on the data yields the values of  $d(\alpha)$  and  $f(\alpha)$  reported in Table 2.

We see that in contrast to the behaviour of  $b(\alpha)$ ,  $f(\alpha)$  increases with  $\alpha$ . This produces a numerical road block in studying the asymptotic behaviour further for  $\alpha = -1.2$  and  $\alpha = -1.4$ . We do not have enough significant digits in our data to measure values of  $B_q^s(v)$  less than  $< e^{-14}$ .

For the nonlinear bound state,  $u(x, t)$ , given by (2.2), we have

$$\|u(\cdot, t)\|_{L^2}^2 = 2(\lambda - |q|).$$

Hence, the behaviour of  $B_q^s(v)$  (see (2.4) and Table 2) shows that  $\lambda$  approaches  $q$  at an exponential rate as  $v \rightarrow \infty$ . We note that for  $\lambda$  very close to  $|q|$ , (2.2) is approximately<sup>2</sup>

$$u(x, t) \approx e^{i\lambda^2 t/2} \sqrt{2} \left(1 - \frac{|q|}{\lambda}\right) \lambda e^{-\lambda|x|} \approx e^{iq^2 t/2} \sqrt{2} \left(1 - \frac{|q|}{\lambda}\right) |q| e^{-|qx|}$$

which is a multiple of the eigenstate (2.1).

Given that the interaction with the delta potential is dominated by the linear part of the equation, we expect the trapped state will, immediately after interaction, resemble a linear eigenstate that will then resolve on a longer time scale to a nonlinear bound state of the form (2.2). It is thus perhaps more appropriate to reverse the heuristics: Given a very small amplitude  $A$ , if we set

$$\lambda = |q| \left(1 - \frac{A}{\sqrt{2}}\right)^{-1},$$

we obtain that the eigenstate of  $H_q$  with amplitude  $A$  is close to  $u(x, t)$  given by (2.2), that is,

$$(2.5) \quad Ae^{iq^2 t/2} e^{-|qx|} \approx u(x, t) \text{ solving (2.2)}$$

It is reasonable to expect that the nonlinear bound state ultimately selected from an immediate post-interaction eigenstate of the *linear* operator  $H_q$ , is “close”, in the sense of (2.5), to the starting eigenstate of  $H_q$ , and indeed, the numerics point in this direction. The first frame of Fig.5 shows for a typical case ( $\alpha = -0.6$ ,  $v = 2$ ) that a stable trapped mass is selected within a reasonable amount of time following the interaction and there is little evidence of mass being radiated away from the origin.

**2.2. Resolution of outgoing waves.** The stabilization of solitons described in (1.11) (and in a slightly weaker form rigorously in [10, Theorem 2]) occurs over long time intervals – see the comment at the end of §4.

Hence for the calculation of the amplitudes  $A_T$  and  $A_R$  in (1.11) we must alter our approach. We begin by solving the nonlinear equation (1.3). However, we also measure the  $L^2$  difference between the solution at every time step and the expected profile given by

$$\exp(ivx + it(1 - v^2)/2)[t_q(v)\operatorname{sech}(x - x_0 - vt) + r_q(v)\operatorname{sech}(x + x_0 + vt)].$$

Shortly after the time of interaction with the delta potential, we see this difference attains a minimum. At this time, we save the computed solution,  $u(x)$ , and continue to solve forward in time. As we solve forward, we compute

$$\|\operatorname{NLS}_q(t)u - \operatorname{NLS}_0(t)u\|_{L_x^2}.$$

---

<sup>2</sup>This is obtained using the two approximations  $\tanh x \approx 1 - 2e^{-2x}$  and  $\operatorname{sech} x \approx 2e^{-x}$  for  $x$  large.

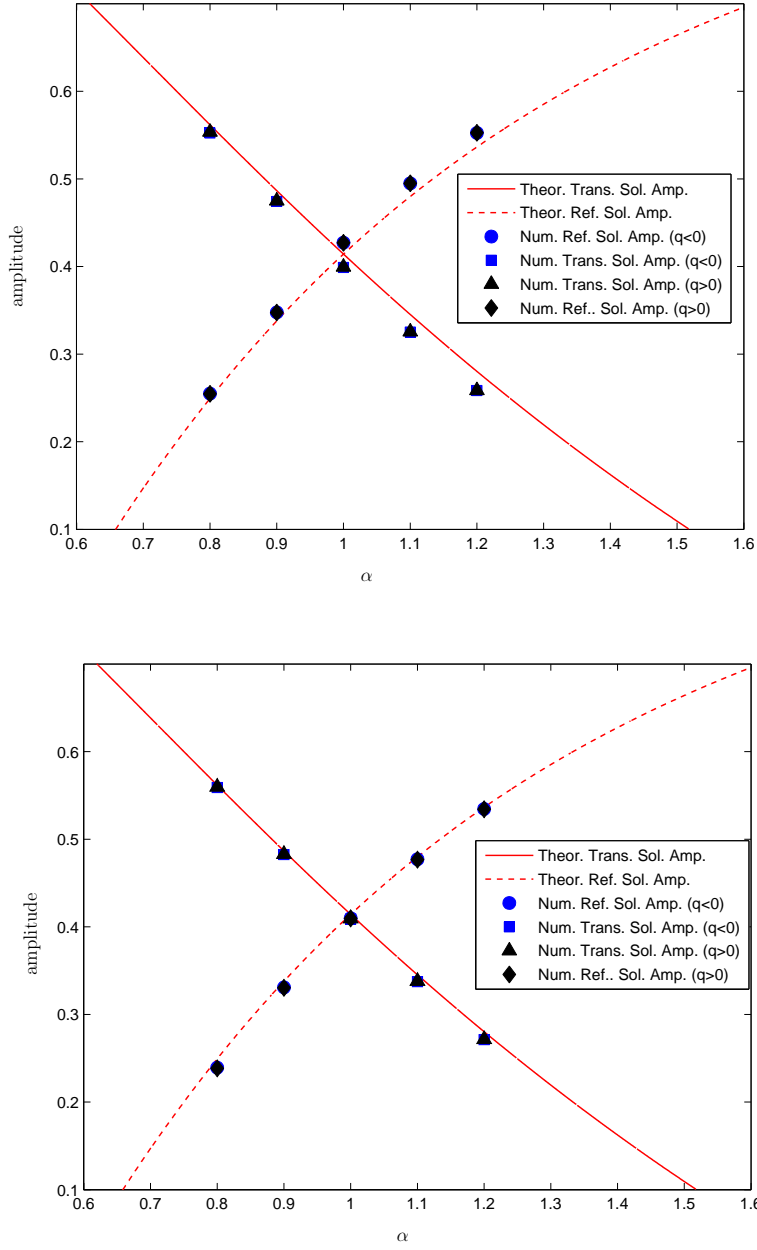


FIGURE 6. A comparison of theory with numerically computed soliton parameters  $A_R$  and  $A_T$ . The first plot is for velocity 3; the second, which shows a better agreement, is for velocity 10. Note here we are plotting *amplitudes*, as opposed to fraction of the total *mass* as in Fig.3.

Since this norm remains negligible we switch to the analysis of the simpler solution of the (1.2),  $\text{NLS}_0(t)u$ .

More precisely, we truncate the solution on both sides of the delta to give two sets of initial data. We then perform a phase shift in order to give each piece a zero velocity. They are then embedded at the center of a very large grid with zeroes outside their computed ranges. From here, we solve forward on this larger grid using  $\text{NLS}_0(t)$  in order to observe the amplitude stabilization predicted by (1.11). The grid is chosen large enough so that several amplitude oscillations can occur without interference from accumulated errors at the boundary. Though the amplitude continues to oscillate, we time average the amplitudes until we see stabilization.

It is these time averages over significantly large intervals that are reported in Fig.6. We see a clear agreement with (1.11) especially for the higher velocity. However, the theoretically predicted thresholds for the formation of the reflected and transmitted solitons (1.12) are hard to verify numerically.

**2.3. Confirmation of the free NLS asymptotics for initial data  $\alpha \text{sech} x$ .** We now turn to the matter of propagating initial data  $\alpha \text{sech} x$  according to  $i\partial_t u + \frac{1}{2}\partial_x^2 u + |u|^2 u$ , which has been explored analytically via the inverse scattering method in [10, Appendix B]. Fig.7 reports the results of an experiment with  $\alpha = 0.8$ . The first panel depicts the time evolution of the amplitude at the spatial origin,  $|u(0, t)|$ , and the second panel depicts the deviation of the time evolution of the phase at the spatial origin from that of the soliton  $(2\alpha - 1)e^{i(2\alpha - 1)^2 t/2} \text{sech}((2\alpha - 1)x)$ . The amplitude appears to be converging to the theoretically expected value of  $2\alpha - 1 = 0.6$  and the phase deviation appears to be converging to the expected value of  $\varphi(0.8) = 0.045$ .

In regard to the phase computation, it should be noted that although this experiment was performed on a  $(x, t)$  grid of size  $15000 \times 20000$  with spatial extent  $-600 \leq x \leq 600$ , the reported phase deviation is the difference of two numbers on the order of 100 and the obtained values are three orders of magnitude smaller. This opens a possibility of an inaccuracy of this long-time computation.

### 3. NUMERICAL METHODS

In this section we outline numerical methods used to produce the results described in §2. We discretize our equation,

$$\begin{aligned} iu_t + u_{xx} + |u|^2 u - q\delta_0(x)u &= 0, \\ u(0, x) &= u_0, \end{aligned}$$

using a finite element scheme in space and the standard midpoint rule in time. Just as the equation itself this method is  $L^2$  conservative. A finite difference scheme can also be implemented with an approximate delta function, but then convergence must be determined in terms of finer meshes as well as more accurate delta function approximations. In finite

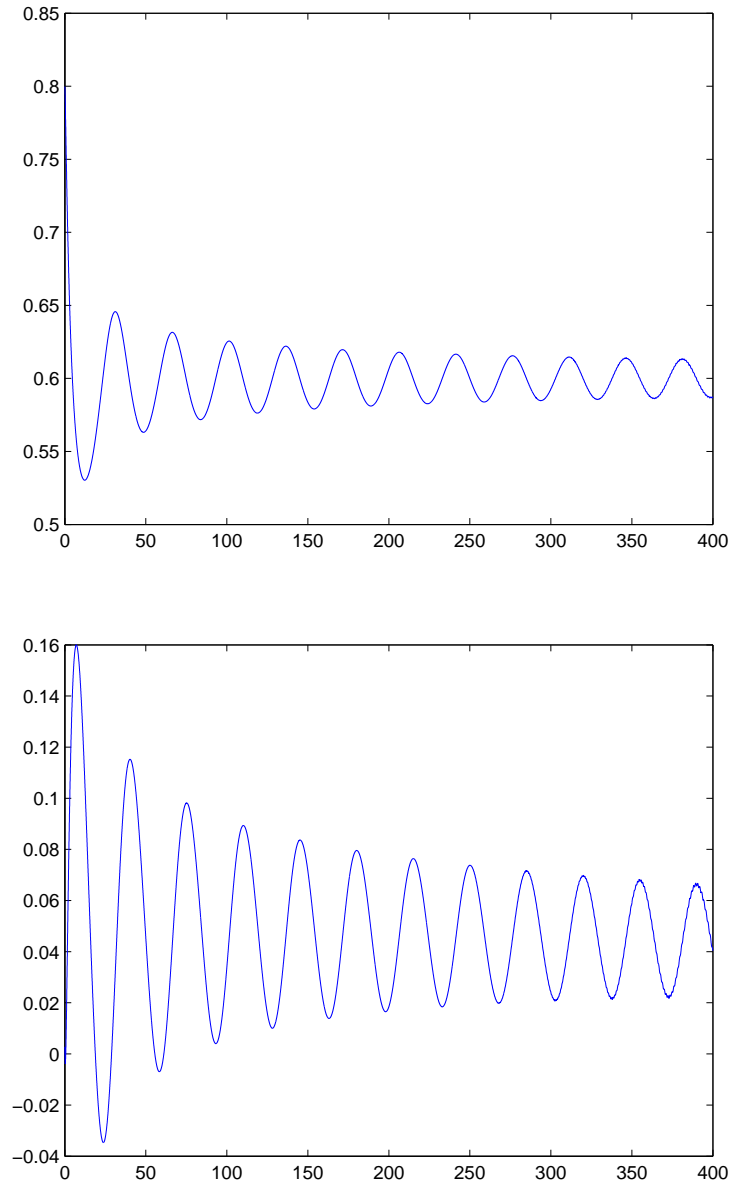


FIGURE 7. Two plots depicting the amplitude and phase of  $u(0, t)$  for the free equation with initial data  $0.8\text{sech}x$ .

element methods the inherent integration allows us to directly incorporate the delta function into the discretization of the problem. A similar scheme was implemented without potential in [2], where the blow-up for NLS in several dimensions was analyzed.

We review the method here and describe how to discretize the delta potential. Note that we require the spatial grid to be large enough to insure negligible interaction with the boundary. For the convergence of such methods without potentials see the references in [2].

We select a symmetric region about the origin,  $[-R, R]$ , upon which we place a mesh of  $N$  elements. The standard hat function basis is used in the Galerkin approximation. We allow for a finer grid in a neighbourhood of length 1 centered at the origin to better study the effects of the interaction with the delta potential. In terms of the hat basis the problem becomes:

$$\begin{aligned} \langle u_t, v \rangle + i \langle u_x, v_x \rangle / 2 - i \langle |u|^2 u, v \rangle + i q u(0) v(0) &= 0, \\ u(0, x) &= u_0, \quad u(t, x) = \sum_v c_v(t) v, \end{aligned}$$

where  $\langle \cdot, \cdot \rangle$  is the standard  $L^2$  inner product,  $v$  is a basis function and  $u, u_0$  are linear combinations of the  $v$ 's. We remark that since  $v$ 's are continuous the pairing of  $uv$  with the delta function is justified.

Since the  $v$ 's are hat functions, we have created a tridiagonal linear system with one contribution to the central element resulting from the delta function. Let  $h_t > 0$  be a uniform time step, and let

$$u_n = \sum_v c_v(nh_t) v,$$

be the approximate solution at the  $n$ th time step. Implementing the midpoint rule in time, the system becomes:

$$\begin{aligned} \langle u_{n+1} - u_n, v \rangle + i h_t \langle ((u_{n+1} + u_n)/2)_x, v_x \rangle + i h_t q (u_{n+1}(0) + u_n(0)) v(0) / 2 \\ = i h_t \langle |u_{n+1} + u_n|^2 (u_{n+1} + u_n)/2, v \rangle, \quad u_0 = \sum_v \alpha_v v, \end{aligned}$$

By defining

$$y_n = (u_{n+1} + u_n)/2,$$

we have simplified our system to:

$$\langle y_n, v \rangle + i \frac{h_t}{4} \langle (y_n)_x, v_x \rangle + i \frac{h_t q}{2} y_n(0) v(0) = i \frac{h_t}{2} \langle |y_n|^2 y_n, v \rangle + \langle u_n, v \rangle.$$

An iteration method from [2] is now used to solve this nonlinear system of equations. To wit,

$$\langle y_n^{k+1}, v \rangle + i \frac{h_t}{4} \langle (y_n^{k+1})_x, v_x \rangle + i \frac{h_t q}{2} y_n^{k+1}(0) v(0) = i \frac{h_t}{2} \langle |y_n^k|^2 y_n^k, v \rangle + \langle u_n, v \rangle.$$

We take  $y_n^0 = u_n$  and perform three iterations in order to obtain an approximate solution.

The measure of success of this method is indicated by the agreement of the computed solutions and the exact solutions such as (1.1), and more remarkably by the agreement with the inverse scattering method – see §2.3 above. When the delta potential is present ( $q \neq 0$ ) the  $L^2$  norm remains essentially constant as predicted by theory.

## 4. REVIEW OF THEORETICAL METHODS

The theoretical results are proved in [10] in the case of a positive coupling constant, that is for  $q > 0$ . The asymptotic formulæ (1.7) and (1.11) are obtained rigorously for times

$$(4.1) \quad \frac{|x_0|}{v} + v^{-1+\epsilon} \leq t \leq \epsilon \log v,$$

and with the error term  $\mathcal{O}_{L^2}(v^{-2})$  replaced by  $\mathcal{O}_{L^2}(v^{-(1-3\epsilon)/2})$  for any  $\epsilon > 0$ , provided that  $x_0$ , the center of the initial soliton, satisfies

$$x_0 < -v^\epsilon.$$

The starting point of the argument is the observation that the *Strichartz estimates* for  $H_q$  hold uniformly in  $q \geq 0$ . Strichartz estimates for dispersive equations [6] describe joint space-time decay properties of solutions and are crucial in the control of interaction terms in nonlinear equations.

More precisely, for the problem

$$(4.2) \quad i\partial_t u(x, t) + \frac{1}{2}\partial_x^2 u(x, t) - q\delta_0(x)u(x, t) = f(x, t), \quad u(x, 0) = u_0(x).$$

they generalize the well known energy inequality:

$$\|u\|_{L_t^\infty L_x^2} \leq C\|u_0\|_{L^2} + C\|f\|_{L_t^1 L_x^2},$$

where, for  $p \neq \infty$ ,

$$\|u\|_{L_t^p L_x^r} = \left( \int \left( \int |u(x, t)|^r dx \right)^{\frac{p}{r}} dt \right)^{\frac{1}{p}}.$$

The Strichartz estimates allow more general exponents  $p$  and  $r$  and, which is essential to us, they hold with constants  $C = C(p, r, \tilde{p}, \tilde{r})$  independent of  $q$ :

$$(4.3) \quad \|u\|_{L_t^p L_x^r} \leq C\|u_0\|_{L^2} + C\|f\|_{L_t^{\tilde{p}} L_x^{\tilde{r}}},$$

$$2 \leq p, r \leq \infty, \quad 1 \leq \tilde{p}, \tilde{r} \leq 2, \quad \frac{2}{p} + \frac{1}{r} = \frac{1}{2}, \quad \frac{2}{\tilde{p}} + \frac{1}{\tilde{r}} = \frac{5}{2},$$

see [10, Proposition 2.2].

We also recall how the reflection and transmission coefficients defined in §1 for stationary scattering enter in time evolutions: for smooth  $\psi$  vanishing outside of  $[-b, -a]$ ,  $0 < a < b$ , we have

$$e^{-itH_q}[e^{ixv}\psi(x)](x) =$$

$$\begin{cases} r(v)e^{-itH_0}[e^{-ixv}\psi(-x)](x) + e^{-itH_0}[e^{ixv}\psi(x)](x) + e(x, t), & x < 0, \\ t(v)e^{-itH_0}[e^{ixv}\psi(x)](x) + e(x, t), & x > 0, \end{cases}$$

where

$$\|e(x, t)\|_{L_x^2} \leq \frac{1}{v}\|\partial_x \psi\|_{L^2}$$

uniformly in  $t$  – see [10, Lemma 2.4].

To describe the proof of weaker versions of (1.7) and (1.11) it will be useful to denote by

$$\text{NLS}_q(t)\varphi(x) = u(x, t)$$

the solution to

$$i\partial_t u + \frac{1}{2}\partial_x^2 u - q\delta_0(x)u + |u|^2 u = 0, \quad u(x, 0) = \varphi(x).$$

When  $q > 0$  we refer to  $\text{NLS}_q(t)\varphi$  as the “perturbed nonlinear flow” and when  $q = 0$ , as the “free nonlinear flow”. Similarly  $\exp(-itH_q)\varphi$  for  $q > 0$  is the “perturbed linear flow”, and  $\exp(-itH_0)\varphi$  is the “free linear flow”.

As discussed in Sect.1 we are interested in

$$u(x, t) = \text{NLS}_q(t)u_0(x), \quad u_0(x) = e^{ixv} \text{sech}(x - x_0), \quad v \gg 1, \quad x_0 \leq -v^\epsilon, \quad 0 < \epsilon < 1.$$

The proof of (1.7) and (1.11) (in the time interval (4.1) and with the error term  $\mathcal{O}_{L^2}(v^{-2})$  replaced by  $\mathcal{O}_{L^2}(v^{-(1-3\epsilon)/2})$ ) proceeds in four phases.

**Phase 1 (Pre-interaction).** Consider  $0 \leq t \leq t_1$ , where  $t_1 = |x_0|/v - v^{-1+\epsilon}$  so that  $x_0 + vt_1 = -v^\epsilon$ . The soliton has not yet encountered the delta obstacle and propagates according to the free nonlinear flow

$$(4.4) \quad u(x, t) = e^{-itv^2/2} e^{it/2} e^{ixv} \text{sech}(x - x_0 - vt) + \mathcal{O}(qe^{-v^\epsilon}), \quad 0 \leq t \leq t_1.$$

The analysis here is valid provided  $v$  is greater than some absolute threshold (independent of  $q$ ,  $v$ , or  $\epsilon$ ). But if we further require that  $v$  be sufficiently large so that

$$v^{-3/2} e^{v^\epsilon} \geq q/v,$$

then

$$qe^{-v^\epsilon} \leq v^{-1/2} \leq v^{-(1-\epsilon)/2}.$$

This is the error that arises in the main argument of Phase 2 below.

**Phase 2 (Interaction).** Let  $t_2 = t_1 + 2v^{-1+\epsilon}$  and consider  $t_1 \leq t \leq t_2$ . The incident soliton, beginning at position  $-v^\epsilon$ , encounters the delta obstacle and splits into a transmitted component and a reflected component, which by time  $t = t_2$ , are concentrated at positions  $v^\epsilon$  and  $-v^\epsilon$ , respectively. More precisely, at the conclusion of this phase (at  $t = t_2$ ),

$$(4.5) \quad \begin{aligned} u(x, t_2) = & t(v) e^{-it_2 v^2/2} e^{it_2/2} e^{ixv} \text{sech}(x - x_0 - vt_2) \\ & + r(v) e^{-it_2 v^2/2} e^{it_2/2} e^{-ixv} \text{sech}(x + x_0 + vt_2) \\ & + \mathcal{O}(v^{-\frac{1}{2}(1-\epsilon)}) \end{aligned}$$

This is the most interesting phase of the argument, which proceeds by using the following three observations

- The perturbed nonlinear flow is approximated by the perturbed linear flow for  $t_1 \leq t \leq t_2$ .



- The perturbed linear flow is split as the sum of a transmitted component and a reflected component, each expressed in terms of the free linear flow of soliton-like waveforms.
- The free linear flow is approximated by the free nonlinear flow on  $t_1 \leq t \leq t_2$ . Thus, the soliton-like form of the transmitted and reflected components obtained above is preserved.

The brevity of the time interval  $[t_1, t_2]$  is critical to the argument, and validates the approximation of linear flows by nonlinear flows. It is here that we used the independence of  $q > 0$  in (4.3).

**Phase 3 (Post-interaction).** Let  $t_3 = t_2 + \epsilon \log v$ , and consider  $[t_2, t_3]$ . The transmitted and reflected waves essentially do not encounter the delta potential and propagate according to the free nonlinear flow,

$$(4.6) \quad \begin{aligned} u(x, t) = & e^{-itv^2/2} e^{it_2/2} e^{ixv} \text{NLS}_0(t - t_2)[t(v) \text{sech}(x)](x - x_0 - tv) \\ & + e^{-itv^2/2} e^{it_2/2} e^{-ixv} \text{NLS}_0(t - t_2)[r(v) \text{sech}(x)](x + x_0 + tv) \\ & + \mathcal{O}(v^{-\frac{1}{2}(1-3\epsilon)}), \quad t_2 \leq t \leq t_3 \end{aligned}$$

This is proved by a perturbative argument that enables us to evolve forward a time  $\epsilon \log v$  at the expense of enlarging the error by a multiplicative factor of  $e^{\epsilon \log v} = v^\epsilon$ . The error thus goes from  $v^{-(1-\epsilon)/2}$  at  $t = t_2$  to  $v^{-(1-\epsilon)/2+\epsilon}$  at  $t = t_3$ .

**Phase 4 (Soliton resolution).** The last phase uses (4.6) and the following result based on inverse scattering method:

$$(4.7) \quad \text{NLS}_0(\alpha \text{sech}) = \begin{cases} e^{i\varphi(\alpha)} \text{NLS}_0((2\alpha - 1) \text{sech}((2\alpha - 1)\bullet)) + \mathcal{O}_{L^\infty}(t^{-\frac{1}{2}}) & 1/2 < \alpha < 1, \\ \mathcal{O}_{L^\infty}(t^{-\frac{1}{2}}) & 0 < \alpha < 1/2, \end{cases}$$

where

$$\varphi(\alpha) = \int_0^\infty \log \left( 1 + \frac{\sin^2 \pi \alpha}{\cosh^2 \pi \zeta} \right) \frac{\zeta}{\zeta^2 + (2\alpha - 1)^2} d\zeta, \quad 1/2 < \alpha < 1,$$

see [10, Appendix B] for the proof and references. The crucial part of the argument involves an evaluation of the transmission and reflection coefficients for the Zakharov-Shabat system  $L\psi = \lambda\psi$ ,

$$L = -iJ\partial_x + iJQ, \quad Q = Q(t, x) = \begin{bmatrix} 0 & \alpha \text{sech} x \\ -\alpha \text{sech} x & 0 \end{bmatrix}, \quad J = \begin{bmatrix} -1 & 0 \\ 0 & 1 \end{bmatrix}.$$

That is done by a well known computation [14],[13, Sect.3.4] which reappears in many scattering theories, from the free  $S$ -matrix in automorphic scattering, to Eckart barriers in quantum chemistry. We quote the results:

$$t(\lambda) = \frac{\Gamma(\frac{1}{2} + \alpha - i\lambda) \Gamma(\frac{1}{2} - \alpha - i\lambda)}{\Gamma(\frac{1}{2} - i\lambda)}, \quad b(\lambda) = i \frac{\sin \pi \alpha}{\cosh \pi \lambda}, \quad r(\lambda) = b(\lambda) t(\lambda).$$

The pole of  $t(\lambda)$  in  $\text{Im } \lambda > 0$  determines the soliton appearing in (4.7). We refer to [10, Appendix B] for a detailed discussion. We only mention that the long time asymptotics in the case of defocusing NLS [7] show that the error estimate  $\mathcal{O}_{L^\infty}(t^{-1/2})$  is optimal and the stabilization to the soliton occurs over a long time.

ACKNOWLEDGMENTS. We would like to thank V. Dougalis, J. Wilkening, J. Strain, and M. Weinstein for helpful discussions during the preparation of this paper. The work of the first author was supported in part by an NSF postdoctoral fellowship, and that of the second and third author by NSF grants DMS-0354539 and DMS-0200732.

## REFERENCES

- [1] U. Al Khawaja, H.T.C. Stoof, R.G. Hulet, K.E. Strecker, and G.B. Partridge, *Bright Soliton Trains of Trapped Bose-Einstein Condensates*, Phys. Rev. Lett. **89**(2002), 200404-
- [2] G.D. Akrivis, V. A. Dougalis, O. A. Karakashian, and W. R. McKinney, *Numerical approximation of blow-up of radially symmetric solutions of the nonlinear Schrödinger equation*, SIAM J. Sci. Comput. **25**(2003), no. 1, 186-212.
- [3] D. Braess, *Finite Elements: Theory, fast solvers, and applications in solid mechanics*, Cambridge University Press, 1997.
- [4] J. C. Bronski and R. L. Jerrard, *Soliton dynamics in a potential*, Math. Res. Lett. **7**(2000), 329-342.
- [5] X.D. Cao and B.A. Malomed, *Soliton-defect collisions in the nonlinear Schrödinger equation*, Physics Letters A **206**(1995), 177-182.
- [6] T. Cazenave, *Semilinear Schrödinger equations*. Courant Lecture Notes in Mathematics, **10**, American Mathematical Society, Providence, 2003.
- [7] P.A. Deift, A.R. Its, and X. Zhou, *Long-time asymptotics for integrable nonlinear wave equations*, in *Important developments in soliton theory*, 181-204, Springer Ser. Nonlinear Dynam., Springer, Berlin, 1993.
- [8] A. Floer and A. Weinstein, *Nonspreading wave packets for the cubic Schrödinger equation with a bounded potential*, J. Funct. Anal. **69**(1986), 397-408.
- [9] R.H. Goodman, P.J. Holmes, and M.I. Weinstein, *Strong NLS soliton-defect interactions*, Physica D **192**(2004), 215-248.
- [10] J. Holmer, J. Marzuola, and M. Zworski, *Fast soliton scattering by delta impurities*, math.AP/0602187, preprint 2006.
- [11] Y.S. Kivshar and B.A. Malomed, *Dynamics of solitons in nearly integrable systems*, Rev. Mod. Phys. **61**(1989), 763-915.
- [12] L.D. Landau and E.M. Lifshitz, *Quantum Mechanics*, 3rd Edition.
- [13] A.I. Maimistov and M. Basharov, *Nonlinear Optical Waves*, Fundamental Theories of Physics, **104** Kluwer Academic Publishers, Dordrecht, Boston, London, 1999
- [14] J.W. Miles, *An envelope soliton problem*, SIAM J. Appl. Math. **41** (1981), no. 2, 227-230.
- [15] V.E. Zakharov and A.B. Shabat, *Exact theory of two-dimensional self-focusing and one-dimensional self-modulation of waves in nonlinear media*, Soviet Physics JETP **34** (1972), no. 1, 62-69.

MATHEMATICS DEPARTMENT, UNIVERSITY OF CALIFORNIA, EVANS HALL, BERKELEY, CA 94720, USA